Dalton Transactions

PERSPECTIVE

View Article Online
View Journal | View Issue

CrossMark click for updates

Cite this: *Dalton Trans.*, 2016, **45**, 9385

Advances in the development of complexes that contain a group 13 element chalcogen multiple bond

Daniel Franz and Shigeyoshi Inoue*

Received 12th April 2016,
Accepted 16th May 2016

DOI: 10.1039/c6dt01413e

www.rsc.org/dalton

Inorganic group 13 element (M) chalcogenides (E) based on the general formular M_2E_3 are ubiquitous in synthesis, catalysis and material science. The parent ME fragment which aggregates to form three dimensional networks in the condensed phase can be expected to exhibit multiple bond character between the elements. Low temperature matrix isolation techniques are required to investigate the nature of this elusive species. An alternate approach for respective studies is the synthesis of electron-precise molecular complexes that contain the ME entity and for which isolation at ambient temperature is possible. This is realized by kinetic stabilization with bulky ligands and thermodynamic stabilization using electron donor, as well as acceptor groups attached to the ME functionality (*i.e.* donor–acceptor stabilization). In this article we revise the literature on complex compounds that exhibit a bonding interaction between a group 13 element atom and a chalcogen atom that is reasonably to be interpreted in terms of a double- or triple bond.

Introduction

Background and scope of this Perspective article

The combination of elements of the group 13 (M) and group 16 (E) mostly results in compounds with the typical stoichiometry M_2E_3 in which the oxidation state +3 is assigned to M and −2 to E. Due to the rather large differences in the electronegativities of M and E, the bonding interaction between the

Institut für Siliciumchemie and Catalysis Research Center, Technische Universität München, Lichtenbergstraße 4, 85748 Garching, Germany. E-mail: s.inoue@tum.de

Daniel Franz

Daniel Franz was born in Ludwigshafen, Germany, in 1981. He studied chemistry at the Goethe University Frankfurt where he received his Ph.D. degree under the guidance of Prof. Matthias Wagner in 2012. Following this he moved to the Technische Universität Berlin to carry out postdoctoral studies in the group of Prof. Shigeyoshi Inoue. Today he is pursuing his research interests in coordination chemistry of group 13 and 14 elements at the Technische Universität München under the supervision of Prof. Inoue.

Shigeyoshi Inoue

Shigeyoshi Inoue received his B.S. (2003), M.Sc. (2005), and Ph.D. (2008) from the University of Tsukuba under the supervision of Prof. Akira Sekiguchi. After a Humboldt postdoctoral fellowship and a JSPS postdoctoral fellowship with Prof. Matthias Drieß at the Technische Universität Berlin, in 2010 he began his independent career at the TU Berlin as a Sofia Kovalevskaja Professor. Since 2015 he has been a W2-Tenure Track Professor for Silicon Chemistry at the Technische Universität München. His research interests focus on the investigation of the synthesis and reactivity of low-valent main group compounds with the goal of finding novel applications.

atoms exhibits high ionic character and they form aggregates of high lattice energy in the solid state. A variety of applications in chemical transformation, catalysis, as well as material science have been found for the compound class of group 13 element chalcogenides.[1] Low-temperature matrix isolation techniques and theoretical studies are required to investigate the lower-aggregated intermediates and the process of how the bulk materials form from these.[2]

The parent entity of these aggregates is the monotopic ME fragment for which it is reasonable to assume a high degree of bonding interaction between the M and the E atom. As an alternate method to matrix isolation techniques, the stabilization of elusive species *via* sophisticated ligand systems (*e.g.* bulky substituents, electron-donor- and electron-acceptor groups) has allowed for the isolation and investigation of well-defined molecular complexes that contain reactive species with pronounced multiple bond character between the elements.[3] Fundamental concepts for the isolation of electron-precise complexes that exhibit a group 13 metal chalcogen interaction with high multiple bond character are illustrated in Fig. 1. By use of a very bulky anionic ligand (R^-) to the metal centre, kinetic stabilization of the ME fragment might be accomplished and the bond order of the metal–chalcogen interaction should approach a value significantly larger than 1 and, thus, correspond to a metal chalcogen double bond (**A**, Fig. 1). As a complement to theoretical investigations (*e.g.* Bond Index, Molecular Orbital Analysis, Natural Resonance Theory) structural information (*i.e.* M–E bond length) and spectroscopic studies (*e.g.* NMR, IR, UV/Vis) may elucidate the multiple-bond properties. In fact, the definition of a multiple bond remains subject to controversy and the transition from a single bond to a double bond and to a triple bond is rather fluent. This is particularly true for strongly polarized bonds because the extend of ionic or covalent contribution to the atom–atom interaction is difficult to assess. However, we presume that the comparison of theoretical and structural parameters between compounds for which the bonding situation is undisputed and those for which a new bonding type may apply is conclusive. Generally, the bonding situation of the metal–chalcogen interaction in complexes of the type R–ME can be described as a composite of the resonance structure R–M=E (**A**) and the zwitterionic forms $R-{}^{+}M-E^{-}$ (**A′**), as well as $R-{}^{-}M\equiv E^{+}$ (**A″**, Fig. 1).

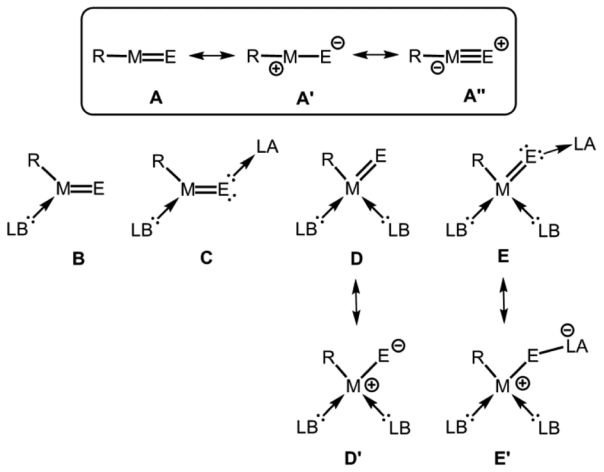

Fig. 1 The parent group 13 element (M) chalcogen (E) double bond species (**A**) and conceivable concepts for its thermodynamic (electronic) stabilization (**B**–**E**), as well as selected resonance structures (**A′**, **A″**, **D′**, **E′**; R = anionic substituent, LB = Lewis base, LA = Lewis acid).

Since the parent R–M=E group is a Lewis acid base pair that is prone to self-quenching by head-to-tail aggregation thermodynamic (*i.e.* electronic) stabilization may be required which is achieved by the introduction of an electron-pair donor ligand to the metal centre (**B**, Fig. 1) and capping the chalcogen atom with an electron-pair acceptor (**C**, Fig. 1). Instead of implementing the latter, aggregation could also be hampered by an additional Lewis base attached to the group 13 metal centre in order to decrease the intrinsic electron-deficiency of the otherwise only three-coordinate group 13 element atom (**D**, Fig. 1). Furthermore, the higher coordination of the metal centre might be complemented by tethering a Lewis acid to the group 16 atom for increased stabilization of the M=E fragment (**E**, Fig. 1). It is feasible that the contribution of zwitterionic canonical structures such as **D′** and **E′** may rise due to the higher coordination number of the group 13 metal centre (Fig. 1).

In this Perspective article, we summarize and assess the present literature on molecular complexes that comprise a group 13 element chalcogen bond with pronounced multiple bond character which allows for the interpretation in terms of a double- or triple bond between the atoms. We focus on classical chemical synthesis in the condensed phase and, hence, gas-phase formation experiments and low temperature matrix isolation techniques are not considered in this paper. Within the subsections of this article the compounds are ordered by chronological appearance in the literature to reflect the evolution of the field in time. Basically, only the non-radioactive elements of group 13 and 16 are considered. A review article from 2010 by Fischer and Power on element–element multiple bonds also includes an outline of group 13 element chalcogen multiple bonds.[3]

Complexes with a boron chalcogen multiple bond

Background. As a consequence of the differences in electronegativities, the bonds between the metalloid boron and chalcogen atoms are strongly polarized and the negative charge density accumulates at the group 16 element (Table 1). In contrast to the heavier homologues of the group 13 family, boron is inclined to be the centre of a trigonal-planar structure motif. This tendency of the boron atom towards three-coordination increases if the ligand atoms compensate the metalloid's electron deficiency *via* π-donation into the unoccupied p-orbital at the boron centre. Thus, one could assume that synthetic access to a B=O double bond should be more simple than for the heavier M=E analogues because π-interaction benefits from the comparably small atomic radii of boron and oxygen (Table 1). However, as apparent from the literature, this is not

Table 1 Covalent radii and values for electronegativities of group 13 and (non-radioactive) group 16 elements[7]

	Covalent radius [Å]	EN (Mulliken)	EN (Pauling)	EN (Allred-Rochow)
B	0.84	1.83	1.88	2.01
Al	1.21	1.37	1.62	1.47
Ga	1.22	1.34	1.77	1.82
In	1.42	n.a.	1.63	1.49
Tl	1.45	n.a.	n.a.	1.44
O	0.66	3.21	3.61	3.50
S	1.05	2.65	2.64	2.44
Se	1.20	2.51	2.46	2.48
Te	1.38	2.34	2.29	2.01

the case. Presumably, the tendency for aggregation inflicted by the strong polarization of the boron–oxygen bond cannot be easily compensated by π-bonding interaction.

Boron oxygen double bond. A pioneering study of Pachaly and West demonstrated the remarkable reactivity of the oxoborane functionality. Irradiation of dioxaboretane **F** affords the transient oxoborane **1** as concluded from its trapping products with oxadisilolane and ketone, respectively (**G**, **H**, Scheme 1).[4] As apparent from the elusive nature of **1** the very bulky supermesityl group does not suffice to kinetically stabilize this highly elusive oxoborane species at ambient temperature. Notably, one would expect partial boron oxygen double- or triple bond character for the three- or two-coordinate boron species, respectively (**F–H**, **1**). In the context of discussing **1**, it is of interest that the related oxoborane (2,4,6-$(CH_3)_3$-C_6H_2)BO was presumed to be produced as an intermediate species in the reaction of the two-coordinate dimesitylborinium ion (2,4,6-$(CH_3)_3$-$C_6H_2)_2B^+$ with carbon dioxide.[5]

In seminal work from 2005, Cowley and coworkers reported the oxoborane complex **2** with a very short B–O distance of 1.304(2) Å (Scheme 2, Fig. 2).[6] For comparison, the sum of the covalent radii of boron and oxygen amounts to 1.50 Å (Table 1).[7] The B–O single bond lengths in representative organoborates (four-coordinate boron centre) range from 1.46 Å to 1.54 Å and tend to decrease with the number of oxygen atoms attached to the metalloid centre.[8] For trigonal-planar organoboranes typical values for B–O bond lengths are found between 1.36 Å and 1.37 Å and the interaction between these atoms often possesses partial double-bond character.[9] A 1,3-diketimino group

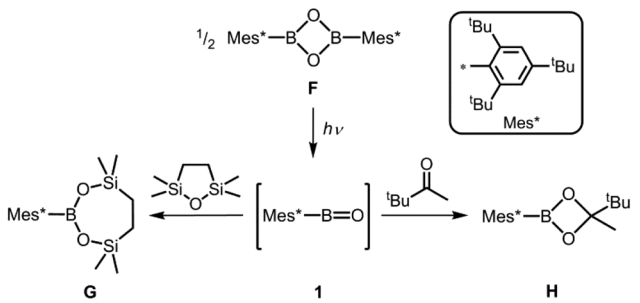

Scheme 1 Irradiation of the dioxaboretane **F** to yield the intermediate oxoborane **1**. Trapping reactions of **1** to form **G** and **H**.

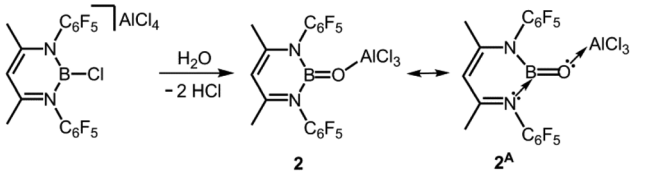

Scheme 2 Synthesis of the oxoborane **2** and the selected resonance structure 2^A.

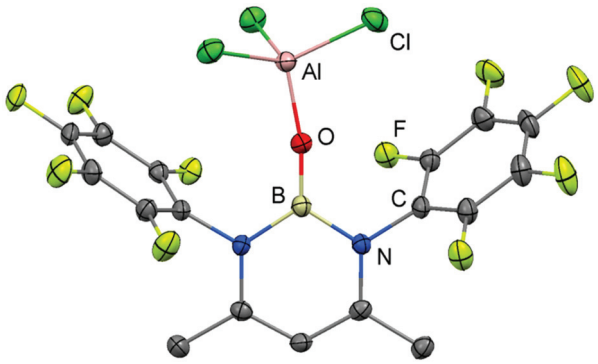

Fig. 2 Ellipsoid plot (50% level) of the molecular structure of **2** in the solid state as derived from XRD analysis. Hydrogen atoms have been omitted.

was used as an ancillary ligand to the boron centre in **2**. The oxygen atom is protected by a capping $AlCl_3$ moiety (Al–O = 1.720(1) Å). Accordingly, the concept of donor–acceptor stabilization of type **C** of the BO fragment is employed as illustrated by resonance structure 2^A (Fig. 1, Scheme 2). Synthetic access to the oxoborane **2** is granted by controlled hydrolysis of the boron halide salt $HC\{C(CH_3)N(C_6F_5)\}_2BCl[AlCl_4]$ (Scheme 2). The authors carried out DFT (Density Functional Theory) calculations on **2**, as well as the model compound **2′** which has no $AlCl_3$ group attached to the oxygen atom and found that the B–O distance decreased only marginally upon removal of the Lewis acid (1.292 Å). However, the molecular orbital analysis revealed significant differences between **2** and **2′** as one would expect. For example, the HOMO (highest occupied molecular orbital) of **2** mainly consists of orbital lobes at the Cl atoms while the HOMO in **2′** principally possesses oxygen lone pair character. The ^{11}B NMR spectroscopic analysis of **2** exhibited a signal at 40.1 ppm.

In 2011 Cui and coworkers enriched the field of oxoborane chemistry by successful isolation of **3** and **4** derived from the hydroxoborane precursor **I** in which a 1,3-diketimino group is employed as a stabilizing ligand to the boron centre (Scheme 3).[10] The Lewis basicity of the oxygen atom is quenched by coordination to a weak Brønsted acid ($[H–NHC]^+$, NHC = N-heterocyclic carbene) or a strong Lewis acid ($B(C_6F_5)_3$, BCl_3), respectively (stabilization concept: **C**, Fig. 1). The bulkiness of the proton donor was varied (**3a**, **3b**) and two different boron-based Lewis acids were implemented (**4a**, **4b**), however, only **3a** and **4a** were structurally characterized *via*

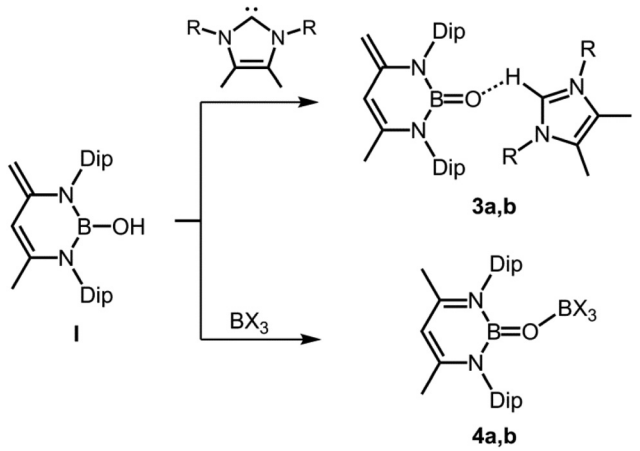

Scheme 3 Syntheses of oxoboranes *via* proton association (**3a,b**) and *via* proton shift (**4a,b**) from hydroxoborane **I** (R = ^{i}Pr for **3a**, Me for **3b**; X = C_6F_5 for **4a**, Cl for **4b**, Dip = 2,6-diisopropylphenyl).

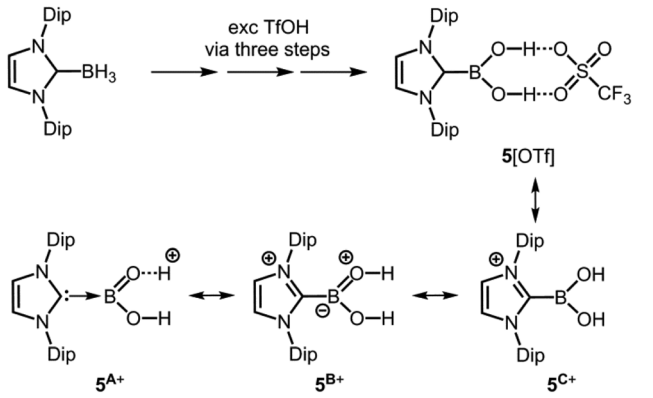

Scheme 4 Conversion of borane–NHC adduct to NHC-stabilized hydroxoborenium salt **5**[OTf] with very short B–O bond lengths. Selected resonance structures of the cation (5^{A+}, 5^{B+} and 5^{C+}; NHC = N-heterocyclic carbene, Dip = 2,6-diisopropylphenyl, Tf = triflyl).

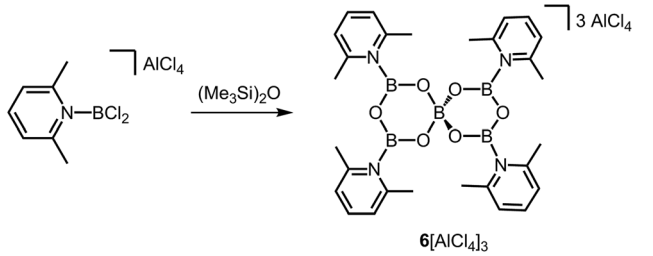

Scheme 5 Conversion of a 2,6-lutidine-stabilized chloroborenium salt to the boroxine salt $\mathbf{6}[AlCl_4]_3$.

XRD (X-ray diffraction) analysis. The B–O distances observed for **3a** amount to 1.287(4) Å and 1.296(3) Å (the compound contains two crystallographically independent molecules in the asymmetric unit), which is slightly shorter than in **2** (*vide supra*). The respective bond lengths for **4a** have values of 1.311(3) Å and 1.314(3) Å (here also: two independent molecules found in the asymmetric unit). The authors reasoned that the marginally longer B–O distances for **4a** are caused by the increased steric congestion of the BO entity inflicted by the $B(C_6F_5)_3$ moiety as compared to the more remote $[H–NHC]^+$ group in **3a**. DFT calculations were carried out on a sterically reduced model compound to **4b** because this complex had not been crystallized and the B–O distance was computed to 1.30308 Å. Interestingly, the B═O double bond length of a model compound to **3** for which the protecting weak Brønsted acid had been removed was calculated to 1.28240 Å which suggests only moderate influence of the O···H interaction in **3** on the degree of its B═O double bond character. Moreover, the application of DFT methods on a sterically reduced model compound to **3** revealed a boron–oxygen π-bonding interaction in the HOMO−7. The ^{11}B NMR chemical shifts of **3a** and **4a** were found at 19.8 ppm and 22.8 ppm, respectively.

Curran and coworkers described the NHC-stabilized dihydroxoborenium salt **5**[OTf] (Scheme 4, Tf = SO_3CF_3) in 2012.[11] The compound was isolated after stepwise treatment of the borane–NHC adduct with an excess of triflic acid and structurally studied by XRD analysis (Scheme 4).[11] The short B–O distances of 1.307(4) Å and 1.310(6) Å suggest that a considerable degree of double bond character can be attributed to the boron–oxygens bonds in $\mathbf{5}^+$. This is illustrated by the canonical forms $\mathbf{5}^{A+}$ and $\mathbf{5}^{B+}$ (Scheme 4) and as apparent from $\mathbf{5}^{A+}$ the bonding situation corresponds to the stabilization concept of type **C** (Fig. 1). A resonance at 22.5 ppm in the ^{11}B NMR spectrum is correlated to this three-coordinate boron cation.

Very short B–O bond lengths (1.296(4) Å and 1.308(4) Å) are observed in the crystal structure of the ionic compound $\mathbf{6}[AlCl_4]_3$ which has been described by Ingleson and coworkers as a tricationic boroxine analogue (Scheme 5).[12] Considering only the crystallographically independent B–O distances of the three-coordinate boron centres in $\mathbf{6}^{3+}$ each B-atom possesses one shorter (*vide supra*) and one longer (1.374(4) Å and 1.378(4) Å) B–O bond length. Presumably, the short B–O bond lengths correlate to the high cationic charge of the complex $\mathbf{6}^{3+}$. In the ^{11}B NMR spectroscopic analysis signals at 25 ppm and 5.2 ppm were attributed to $\mathbf{6}^{3+}$.

In 2013 Robinson and coworkers reported compound **7**[Br] which is a borenium salt reminiscent of **5**[OTf] (Scheme 4, Scheme 6).[13] Though the B–O distances in $\mathbf{7}^+$ (1.339(11) Å and 1.345(11) Å) clearly reside below the typical length of a B–O single bond (*vide supra*) they are longer than in $\mathbf{5}^+$. Accordingly, the double bond character as represented by the canonical forms $\mathbf{7}^{A+}$ and $\mathbf{7}^{B+}$ is probably lower than in $\mathbf{5}^+$ (Scheme 6). However, the structural features of $\mathbf{7}^+$ support the assumption that the introduction of cationic charge to a boron complex may generally strengthen the boron–oxygen interaction as in $\mathbf{5}^+$ and $\mathbf{6}^+$. The ^{11}B NMR chemical shift of $\mathbf{7}^+$ was observed at 26.60 ppm.

Also in 2013 Miyada and Yamashita described the oxoborane ruthenium compound **8** which is derived from its boryl pincer complex precursor by insertion of oxygen into the B–Ru bond (Scheme 7).[14] As a source of oxygen they implemented

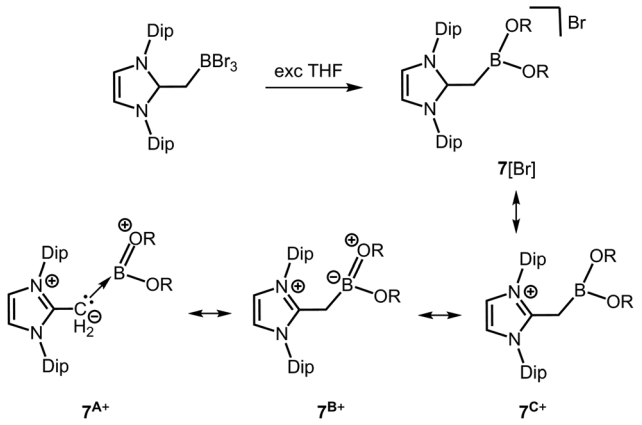

Scheme 6 Reaction of bromoborane–NHO adduct to the alkoxy borenium salt **7**[Br] *via* ether cleavage (NHO = N-heterocyclic olefin, Dip = 2,6-diisopropylphenyl, R = $(CH_2)_4Br$). Selected resonance structures $\mathbf{7}^{A+}$, $\mathbf{7}^{B+}$ and $\mathbf{7}^{C+}$.

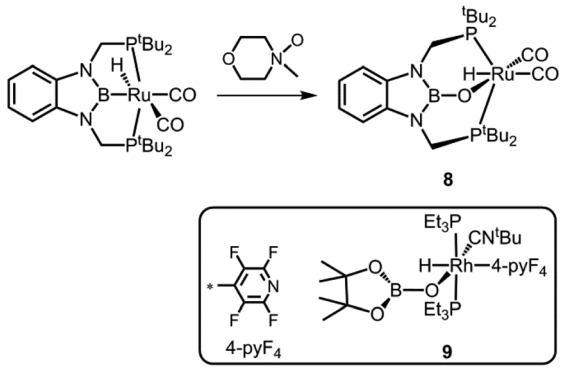

Scheme 7 Synthesis of the oxoborane ruthenium complex **8**. The rhodium congener **9** (boxed).

N-methylmorpholine *N*-oxide. The B–O distance in **8** amounts to 1.329(6) Å and, thus, it is shorter than in $\mathbf{7}^{+}$ but elongated in comparison to the uncharged oxoborane **2**. Interestingly, a WBI (Wiberg Bond Index) of 1.04 was calculated for the boron–oxygen interaction in **8** and this value is considerably higher than expected for a boron oxygen single bond if one takes the strong polarization along the B–O vector into account. As apparent from the direct comparison of the B–N distances in **8** (1.457(7) Å, 1.450(6) Å) with its boryl precursor (1.432(9) Å, 1.436(9) Å) the introduction of the oxygen atom as an additional π-donor substituent weakens the π-interaction between the boron atom and the nitrogen ligands. Notably, compound **8** is related to the oxoborane rhodium complex **9** for which the distance between the boron centre and the rhodium-bonded oxygen atom was observed at 1.328(11) Å (Scheme 7).[15] Compound **8** gave rise to a peak at 22.7 ppm in the ^{11}B NMR spectrum.

In a report from the year 2014 Kinjo and coworkers described the 1,2,3,4-triazaborole-based oxoborane **10** (Scheme 8) in which the oxygen atom is attached to a protecting $AlCl_3$ group, similar to complex **2**.[16] The B–O distance amounts to 1.304(3) Å and the Al–O bond length was determined to 1.7073(16) Å. These values are very similar to **2** for which relevant B=O double bond character has been acknowledged. As apparent from resonance form $\mathbf{10}^{A+}$ concept **C** may apply for the stabilization of the BO fragment (Fig. 1, Scheme 8). For comparison, the hydroxoborane precursor of **10** exhibits a B–O distance of 1.351(7) Å (Scheme 8). Remarkably, a B=O bond length of 1.264 Å was calculated for a model compound of **10** that is free of the $AlCl_3$ moiety. Furthermore, a WBI of 1.07 was reported for the strongly polarized boron–oxygen bond in the optimized structure of **10** and that value is marginally larger than in compound **8**. In the infrared spectroscopic study of **10** a band at 1636 cm^{-1} was assigned to the boron oxygen stretch vibration. Notably, in the ^{11}B NMR spectrum a resonance at 18.9 ppm was attributed to **10**.

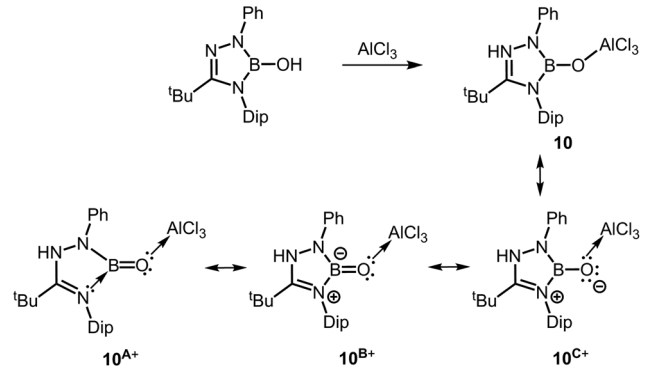

Scheme 8 Synthesis of the oxoborane **10** and selected resonance structures $\mathbf{10}^{A+}$, $\mathbf{10}^{B+}$ and $\mathbf{10}^{C+}$ (Dip = 2,6-diisopropylphenyl).

Boron oxygen triple bond. In 2010 Braunschweig and coworkers published their seminal report on boron–oxygen triple bonds stabilized in the coordination sphere of platinum (**11**, **12**, Scheme 9).[17] The B–O distance of **11** was computed to 1.226 Å (XRD data did not suffice discussion of structural parameters) and the NRT (Natural Resonance Theory) bond order for the boron–oxygen interaction was determined to 2.83 which is a high value if one considers the presumably strong polarization along the B–O vector. Though the presence of the low-coordinate boron species in **11** is not verified by the ^{11}B NMR signal observed at 17 ppm (strong inductive effects will be produced by the adjacent transition metal) the infrared spectroscopic analysis confirmed the strength of the B≡O bond (bands at 1797 cm^{-1} and 1853 cm^{-1}). Notably, these vibrations indicate higher bond energy than observed for the boron oxygen double bond in **10** (band at 1636 cm^{-1}, *vide supra*). DFT methods revealed that the π-MOs in **11** possess considerable overlap between the BO fragment and d-type orbitals at the platinum centre. Interestingly, *via* stepwise addition of $BrSiMe_3$ to **11** it was verified that the terminal oxoborane is in dynamic equilibrium with its bromoboryl precursor (Scheme 9).[17] The conversion of **11** with Bu_4N[SPh] afforded **12** for which a B–O distance of 1.210(3) Å was found *via* XRD analysis (Scheme 9, Fig. 3).[17] The ^{11}B NMR analysis of **12** revealed

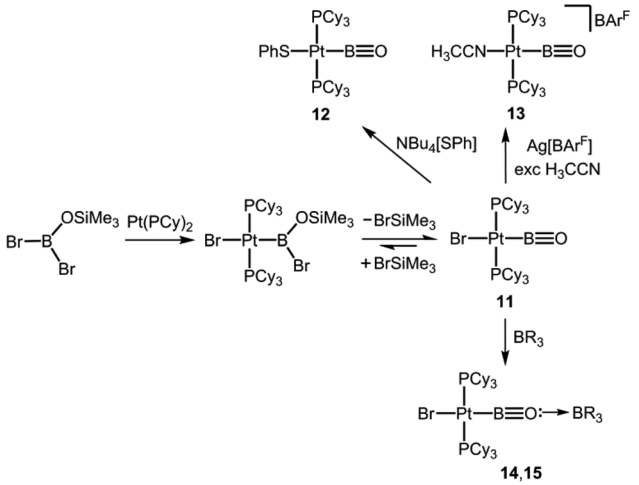

Scheme 9 Oxidative addition of siloxy bromoborane to form a platinum phosphine complex and its conversion to oxoborane **11**. Reactions of **11** to phenylsulfide **12** nitrile complex **13**, as well as the oxoborane adducts **14** and **15** (Cy = cyclohexyl, Ar^F = 3,5-$(CF_3)_2$-C_6H_3, R = Ar^F or C_6F_5).

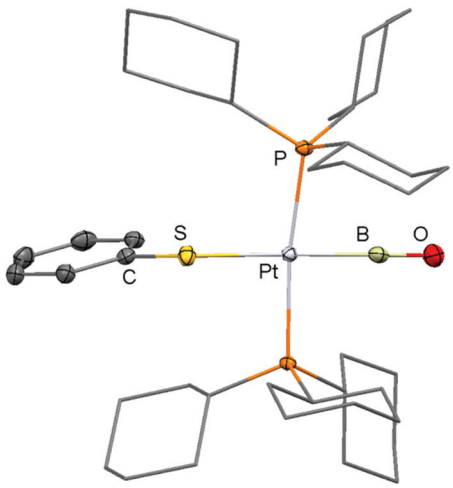

Fig. 3 Ellipsoid plot (50% level) of the molecular structure of **12** in the solid state as derived from XRD analysis. Hydrogen atoms have been omitted. Cyclohexyl groups are depicted as stick model.

a signal at 24 ppm. Further derivatization experiments on **11** resulted in the syntheses of complexes **13–15** (Scheme 9).[18] In addition, a variety of adducts between the platinum oxoboryl system and group 13 metal-based Lewis acids has been reported very recently.[19]

Boron sulfur- and boron selenium double bond. Tokitoh *et al.*, in their seminal work, described the reaction of a dithiastannaboretane (**J**) with 1,3-dienes at elevated temperature which afforded boron–sulfur heterocycles (**K**, Scheme 10).[20] The formation of **K** was reasoned by the intermediate presence of the thioxoborane **16** with a B═S double bond that engages in cycloaddition reactions with the olefin. However, the characterization and isolation of this highly elusive species (**16**) could not be accomplished.

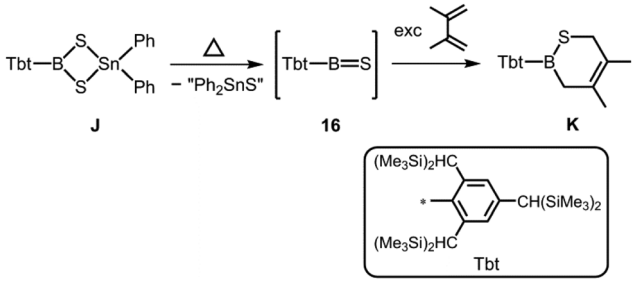

Scheme 10 Formation of thioxoborane intermediate **16** from dithiastannaboretane **J** and its representative trapping product with 2,3-dimethyl-butadiene (**K**).

In 2010 Cui and coworkers presented their study on the 1,3-diketiminato-stabilized thioxoborane **17**, as well as its heavier selenoxoborane congener **18** (Scheme 11).[21] As apparent from the structural formulation the BE entity (E = S or Se) bears two ligands to the metal centre but lacks an additional stabilizing Lewis acid at the chalcogen atom as implemented for the BO moiety in respective oxygen congeners (*vide supra*). Hence, the system corresponds to the concept of type **B** for thermodynamic stabilization as illustrated by the canonical forms $\mathbf{17}^{\mathbf{A}}$ and $\mathbf{18}^{\mathbf{A}}$ (Fig. 1, Scheme 11). Access to these compounds (**17**, **18**) is granted by conversion of the hydridoborane precursor with elemental sulfur or selenium. Interestingly, the reaction runs *via* hydrogen shift from the putative hydrogenchalcogenide intermediate to the backbone of the diketiminato ligand (Scheme 11). The XRD study of the final products showed B–E distances that amount to 1.741(2) Å in **17** and 1.896(4) Å in **18** and for the former the authors pointed out the decrease in the B–S distance as compared to typical three-coordinate boron compounds with a B–SR moiety. The difference in the bond lengths between the analogues (0.155 Å) corresponds to the deviation in the covalent radii (r) of sulfur and selenium (r_S = 1.05 Å, r_{Se} = 1.20 Å).[7] Moreover, the structural parameters of the NBN moiety in **17** and **18** are very similar. Consequently, it is reasonable to assume strong resemblance in the nature of the boron–chalcogen bonds of both compounds. The B–N distances are in a narrow range of 1.48 Å to 1.49 Å. This is increased with respect to 1,3-diketimino boranes with a single bond to a chalcogen atom as the hydroxoborane **I** (Scheme 3, 1.433(5) Å and 1.436(5) Å). This accounts for the higher boron nitrogen dative bond character in **17** and **18** which complies

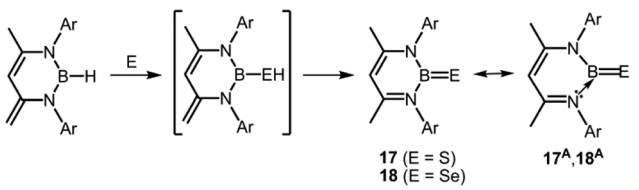

Scheme 11 Reaction of diketimino borane to intermediate hydrogenchalcogenide and its conversion to the thioxoborane **17**, as well as the selenoxoborane **18**. Selected resonance structures $\mathbf{17}^{\mathbf{A}}$ and $\mathbf{18}^{\mathbf{A}}$ (Ar = 2,6-$(CH_3)_2$-C_6H_3).

with the stabilization concept **B** (Fig. 1). For **17** the B═S double bond was verified by Natural Bond Order analysis and Kohn–Sham depictions of the frontier orbitals showed that the HOMO−1 comprises significant contribution from a boron sulfur π bond. In the infrared spectra of **17** and **18** the B═E stretching vibration modes are observed at 1161 cm^{-1} and 1136 cm^{-1}, respectively. The ^{11}B NMR spectrum of **17**, as well as **18** showed a signal at 36.79 ppm and at 40.88 ppm, respectively.

A rare example for the stabilization of a putative boron–sulfur double bond in the coordination sphere of a transition metal was given by the group of Braunschweig in 2013.[22] The metallacycle intermediate **19** was observed *via* NMR spectroscopy in the reaction of a manganese borylene system with triphenylphosphorane sulfide to afford a manganese phosphine complex (in the ^{11}B NMR analysis a broad signal at 88.6 ppm was attributed to **19**; Scheme 12). The resonance structure **19^{A}**, that is an η^2-bonded thioxoborane with a B═S double bond stabilized in the coordination sphere of the transition metal, may have relevant contribution to the bonding situation (Scheme 12). The existence of **19** was supported by DFT calculations, but the compound was not characterized by X-ray diffraction analysis.

We made a contribution to the field by our report on the cationic thioxoborane **20^{+}** in 2014 (Scheme 13, Fig. 4).[23] The XRD analysis revealed a B–S distance of 1.710(5) Å which is even shorter than in **17** (*vide supra*). The calculated Natural Bond Orbital (NBO) charge of +0.634 at the boron atom indicates that **20^{+}** possesses boron-centred cation character as represented by the canonical structure **20^{A+}** (Scheme 13). Moreover, the calculated WBI of 1.739 verifies the B═S double bond nature particularly if one considers the strong polarization along the BS vector (NBO charge at S = −0.578). Accordingly, the HOMO−1 in **20^{+}** is marked by the π bonding interaction between the boron and the sulfur atom whereas HOMO and LUMO comprise the lone pair at the sulfur atom and ligand-centred orbital contributions, respectively (Fig. 5). Notably, the B–N distances in **20^{+}** amount to 1.483(5) Å and 1.493(5) Å and, thus, partial boron nitrogen double bond character is concluded (Fig. 4). *Vice versa* the

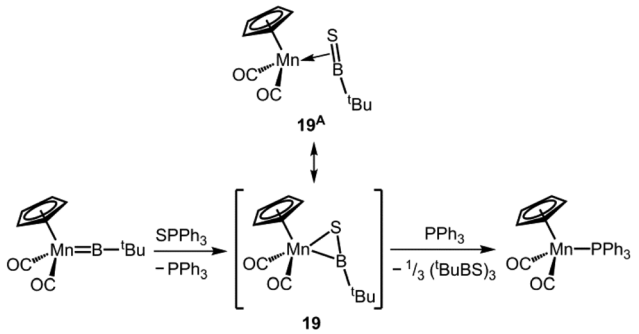

Scheme 12 Reaction of a manganese borylene complex to a manganese phosphine complex *via* the metallacycle intermediate **19** and its resonance structure representing thioxoborane character (**19^{A}**).

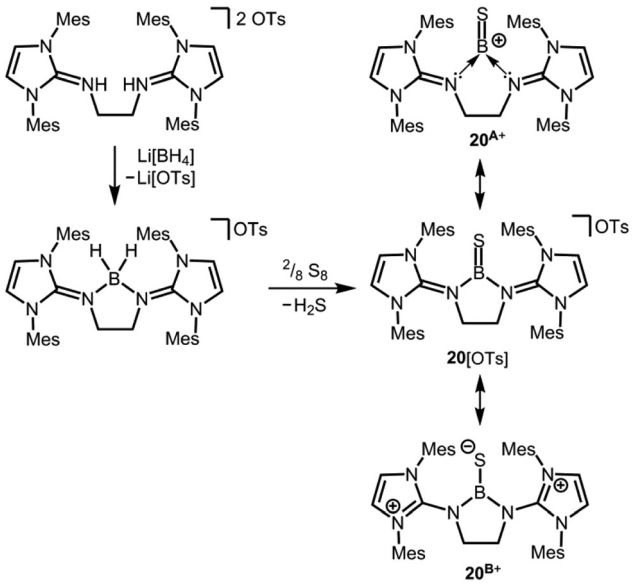

Scheme 13 Synthesis of a dihydridoboronium salt and its conversion to the tosylate salt of the cationic thioxoborane (**20**[OTs]). Selected resonance structures **20^{A+}**, as well as **20^{B+}** (Mes = mesityl, Ts = tosyl).

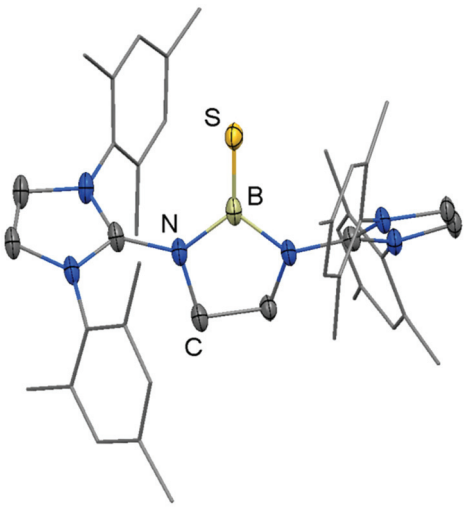

Fig. 4 Ellipsoid plot (30% level) of the molecular structure of **20^{+}** in the solid state as derived from XRD analysis. Hydrogen atoms have been omitted. Mesityl groups are depicted as a stick model.

C–N_{imino} bonds are longer than typically found for C═N double bonds. This accounts for the partial delocalization of positive charge density into the imidazoline rings as represented by the resonance structure **20^{B+}** (Scheme 13). The ^{11}B NMR chemical shift of **20^{+}** was determined to 33.9 ppm.

Singh and coworkers converted a boron dihydride complex with two equivalents of elemental sulfur or selenium to obtain the thioxoborane **21** and the selenoxoborane **22**, respectively (Scheme 14).[24] The bis(phosphoranimino)aminato ligand is a monoanionic system which is less inclined to switch to a dianionic group by proton transfer as observed for the 1,3-diketi-

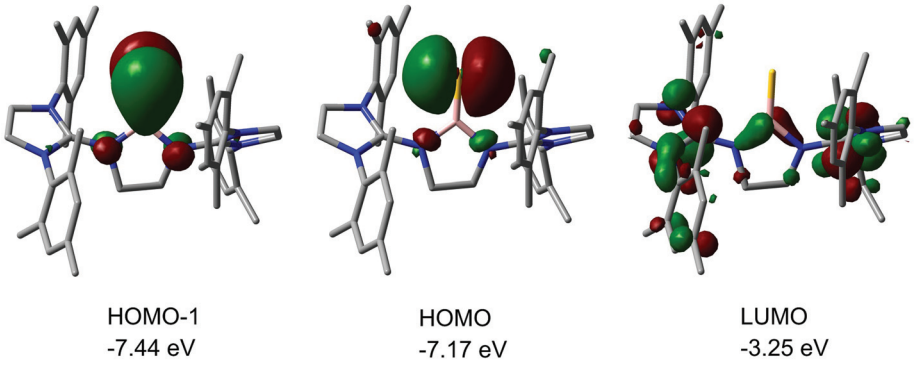

Fig. 5 Kohn–Sham depictions and relative energy levels with occupancy of selected molecular orbitals of $\mathbf{20}^{+}$ (LUMO, HOMO, HOMO–1). Colours: Pink (boron), yellow (sulfur), blue (nitrogen), gray (carbon). Hydrogen atoms omitted.

minato ligand in **17** and **18**. In structural resemblance to these the boron centre in **21** and in **22** is attached to two nitrogen atoms incorporated into a six-membered ring system. The B–S distance of 1.752(5) Å in **21** is slightly elongated in comparison to the B=S double bond in **17**, however, the B–Se bond length of 1.871(5) Å in **22** is decreased with respect to its ketimine congener **18** (1.896(4) Å). Similar to the formation of **17**, **18** and $\mathbf{20}^{+}$ a hydrogenchalcogenide intermediate was presumed for the reaction pathway that leads to **21** and to **22** (Scheme 14; monohydrogensulfide species for **17** and **18**; bis(hydrogensulfide) species for $\mathbf{20}^{+}$, **21** and bis(hydrogenselenide) species for **22**). The three-coordinate borane (**21**, **22**) results from elimination of EH_2 from the four-coordinate species (as in $\mathbf{20}^{+}$) which contrasts the hydrogen shift mechanism involved in the formation of the congeners **17** and **18** (*vide supra*, Schemes 11 and 14). The infrared spectroscopic study of **21** and **22** revealed the stretching vibration modes of the boron chalcogen bonds at 1096 cm^{-1} and 1076 cm^{-1}, respectively. These values are at lower wave number than observed for **17** and **18** (*vide supra*). In the ^{11}B NMR spectroscopic study **21** and **22** produced resonances at 41 ppm and 45.2 ppm, respectively.

Very recently, Cui's group described the desulfination of boron polysulfides to the thioxoborane **23** by means of implementing triphenylphosphine as a chalcogen scavenger (Scheme 15).[25] No structural data was reported for **23**. The compound **23** gave rise to a peak at 50.3 ppm in the ^{11}B NMR spectrum. If one considers that the number of competing π-donor ligands in **23** is decreased with respect to **17**, $\mathbf{20}^{+}$ and **21**, it is reasonable to expect an increased boron sulfur bond order for the compound due to stronger electron donation from a lone pair at the sulfur atom to the boron-centred p-orbital.

Related boron tellurium compounds. There are a number of borane cluster compounds with a boron tellurium interaction.[26] In sharp contrast, molecular electron-precise complexes with a boron–tellurium bond of any type are surprisingly rare. In fact, we found only the $(9\text{-BBN})_2Te$ and $\{(9\text{-BBN})Te\}_2$ as related examples.[27] Due to the unoccupied p-orbital at the boron centre, one would expect partial boron–tellurium double bond character for these compounds to a minor degree, though, the covalent radius of Te is comparably large (Table 1). However, the nature of the interaction was not conclusively elucidated by means of structural or theoretical investigation. Of course, the formation of aggregates in the condensed phase in which the electron deficiency of the boron atom is compensated by intermolecular interaction between the boron- and tellurium centres is feasible, as well. The ^{11}B NMR resonances produced by $(9\text{-BBN})_2Te$ and $\{(9\text{-BBN})Te\}_2$ were observed at 93.5 ppm and 87.0 ppm, respectively.

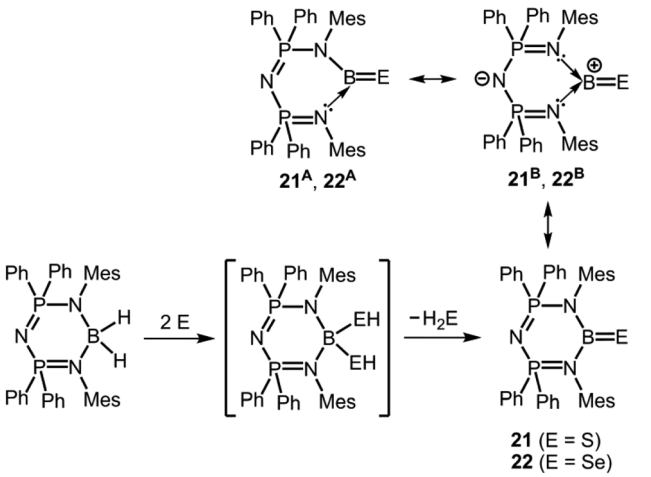

Scheme 14 Conversion of bis(phosphoranimino)amino boron dihydride to the thioxoborane **21**, as well as selenoxoborane **22** *via* a postulated bis(hydrogenchalcogenide) intermediate. Selected resonance structures $\mathbf{21}^{A}$, $\mathbf{22}^{A}$ and $\mathbf{21}^{B}$, $\mathbf{22}^{B}$ (Mes = mesityl).

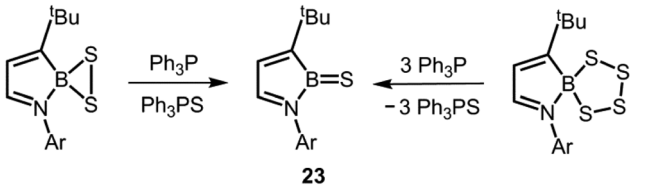

Scheme 15 Synthesis of the thioxoborane **23** *via* desulfination of boron persulfide (left) or boron tetrasulfide (right; Ar = 2,6-$(CH_3)_2$-C_6H_3).

Complexes with an aluminium chalcogen multiple bond

Background. Aluminium is marked by electronegativity values significantly smaller than that of boron (Table 1). As a result, the polarization of aluminium chalcogen bonds is usually stronger in comparison to boron chalcogen bonds and therefore the Lewis acid base pair character of the AlE fragment should be more pronounced, as well (*vide supra*). Moreover, the increased atomic radius of aluminium with respect to boron increases its tendency to form complexes with a higher coordinate metal centre (Table 1). In fact, three-coordinate aluminium complexes with chalcogen substituents at the metal centre have been described in the literature,[28] but they are remarkably rare as compared to trigonal planar boron compounds. As another consequence of aluminium's larger atomic radius, the π-interaction with attached chalcogen atoms is generally weaker than that for boron. Accordingly, related examples with aluminium chalcogen double bond character rather follow the concepts **D** and **E** for thermodynamic stabilization *via* a four-coordinate metal centre (*vide infra*, Fig. 1). In this context, it has to be pointed out that isolated complexes that contain multiple bonds between aluminium atoms or between aluminium and a group 14 or 15 element are surprisingly rare in comparison to its neighbours in the periodic table. A monomeric iminoalane (Al═N double bond) was described by Cui and coworkers.[29] Extensive studies that aimed at the isolation of a dialumene (Al═Al double bond) had been carried out by Power's and by Tokitoh's group, however, only trapping products of this elusive species were isolated.[30] Maybe closest to complexes with Al═Al double bonds are related examples of Power, as well as Pörschke and coworkers who isolated the lithium salts of radical compounds which were described to comprise a one-π-electron bond in addition to the Al–Al single bond.[31]

Aluminium oxygen double bond. In 2002 Roesky and coworkers reported their outstanding study of the monotopic alumoxane **24** (Scheme 16).[32] The metal centre is incorporated into a 1,3-diketimino scaffold and the bonding situation corresponds to the Lewis acid base-stabilization concept **E** as represented by the canonical structure **24^{A}** (Fig. 1, Scheme 16). The remarkably low Al–O distance of 1.659(3) Å is shorter than in typical ditopic aluminium oxygen complexes with a diketiminate ligand and four-coordinate aluminium centres (1.68–1.91 Å).[28e,32,33] It is in the range of aluminium compounds with the very bulky 2,6-ditertbutyl-4-methyl-phenoxide ligand (1.64–1.69 Å) which mark a class of aluminum complexes that often comprise the metal centre in the coordination number three that is scarcely-found for aluminium.[28] Notably, one Al–O distance in a tellurium-bridged ditopic 1,3-diketimino aluminium oxide was determined to 1.588(3) Å.[33c] However, this very short bond length does not imply aluminium oxygen double bond character as obvious from the bonding situation.

Related aluminium sulfur or -selenium compounds. Interestingly, to the best of our knowledge, there are no examples reported for complexes that contain an aluminium and a sulfur or selenium atom that engage in an interaction of considerable double bond character. Several aluminium bis(hydrogensulfide)- and bis(hydrogenselenide) complexes, as well as related hydride hydrogenchalcogenides were described.[33b,34] However, the elimination of H_2S or dihydrogen, respectively, to yield monotopic thioxoalane similar to the formation of thioxoboranes from their boron hydrogensulfide precursors (*vide supra*) has not been reported to date.

Aluminium tellurium double bond. In 2015 we found a ditopic aluminium ditelluride with the chalcogen in the oxidation state −1 that reacts with NHC (L^{Et}, 5 equiv., L^{Et} = 1,3-diethyl-4,5-dimethyl-imidazolin-2-ylidene) in a dehydrogenative redox process.[35] In this process the monotopic aluminium telluride **25** with the chalcogen in the formal oxidation state −2 is furnished along with dihydrogenated NHC ($L^{Et}(H_2)$; Fig. 6, Scheme 17; concept **D**, Fig. 1).[35] The structural study of **25** revealed a remarkably short Al–Te distance of 2.5130(14) Å and DFT calculations determined an enhanced aluminium–tellurium interaction (WBI_{AlTe} = 1.20; NPA charges: Al = +1.24, Te = −0.95; NPA = Natural Population Analysis). Interestingly, the terminal position of the tellurium atom is a very scant structure motif as group 16 atoms commonly assume bridging positions in aluminium chalcogenides. Accordingly, it does not come as a surprise that upon heating a benzene solution

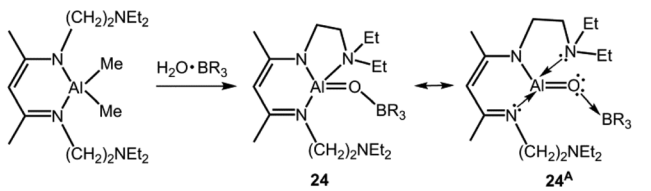

Scheme 16 Conversion of the diketimino dimethylalane to the alumoxane **24** (R = C_6F_5). Selected resonance structure **24^{A}** illustrates the donor–acceptor stabilization mode.

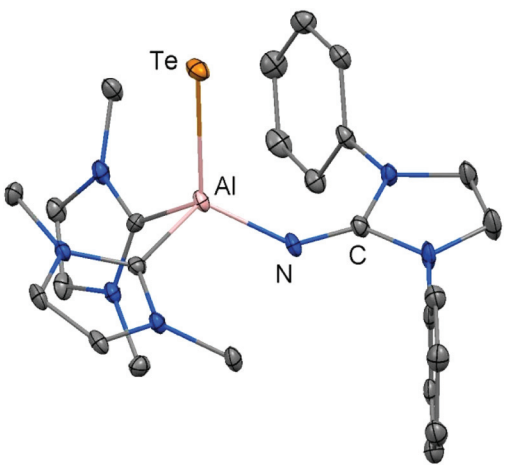

Fig. 6 Ellipsoid plot (30% level) of the molecular structure of aluminium telluride **25** in the solid state as derived from XRD analysis. Hydrogen atoms isopropyl groups and non nitrogen-bonded methyl groups have been omitted.

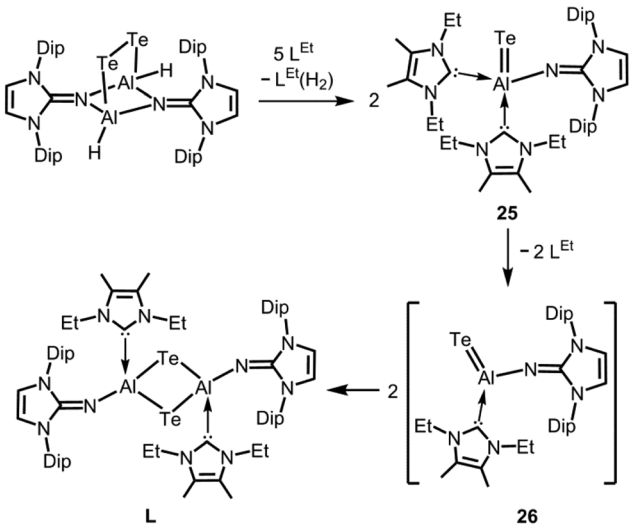

Scheme 17 Reaction of a ditopic aluminium ditelluride to the monotopic aluminium telluride **25** and its thermal transformation to ditopic **L** *via* the calculated intermediate **26** (Dip = 2,6-diisopropylphenyl, L^{Et} = 1,3-diethyl-4,5-dimethyl-imidazolin-2-ylidene).

of **25** to 80 °C one of the two L^{Et} ligands is released. The intermediate $L^{Dip}N(AlTe)L^{Et}$ (**26**, Al–Te = 2.428 Å; L^{Dip} = 1,3-bis(2,6-diisopropylphenyl)-imidazolin-2-ylidene) aggregates to tellurium-bridged **L** and this process was computed by DFT methods (Scheme 17). The XRD analysis of **L** revealed significantly elongated Al–Te distances (2.6143(14) Å, 2.6211(15) Å) and a decreased bond order for the aluminium–tellurium interaction (WBI_{AlTe} = 0.75; NPA charges: Al = +1.21, Te = −0.79) with respect to **25**.[35] Taking into account the salient changes in the Al–Te distances and the values for the WBI_{AlTe} upon transformation of **25** into **L**, the nature of the aluminium–tellurium interaction in **25** was presumed to possess high Al═Te double bond character. This is supported by a pronounced π-symmetric orbital lobe in the HOMO−1 which expands between the aluminium centre and the tellurium atom (Fig. 7). Notably, the aluminium species in **25** is isoelectronic to a sila-acylium ion for which significant Si═O double bond character had been verified by NBO- and NRT analysis, as well as Mayer Bond Index and infrared spectroscopy.[36]

Complexes with a heavier group 13 metal chalcogen multiple bond

Background. The increase in atomic number of the group 13 elements gallium, indium and thallium corresponds to electronegativity values that are mostly higher than found for aluminium (Table 1). Hence, the polarization of the M–E (M = Ga, In, Tl) bonds is generally weaker than for aluminium. Albeit the covalent radius of gallium is very similar to aluminium's the radii of indium and thallium are considerably increased and respective impact on the preferred coordination number (*i.e.* larger) and the π-interaction with chalcogen atoms (*i.e.* weaker) is to be expected (Table 1). Consequently, the tendency to form double-bonded systems is likely to be diminished for indium and thallium. In fact, we found no report for a thallium chalcogen multiple bond in the literature.

Gallium chalcogen double bond. As the only examples for electron-precise complexes that contain a potential gallium chalcogen multiple bond, we found the work of Kuchta and Parkin on the complexes **27–29** with the tris(3,5-ditertbutyl) pyrazolylhydridoborato ligand ($[HB(pz^{tBu})_3]^-$, Scheme 18).[37,38] With regard to the ligand system concept **D** for stabilization of the GaE species would apply. However, if one considers that the electronic nature of the trispyrazolylborato ligand – its complexes are often referred to as "*scorpionates*" – has been compared to the cyclopentadienide anion unambiguous assignment according to the concepts for thermodynamic stabilization as outlined in this introduction is difficult.[39] Compounds **27–29** derive from direct conversion of the trigonal pyramidal gallium(I) *scorpionate* $HB(pz^{tBu})_3Ga$ with the respective chalcogen in elemental form (Scheme 18).[37,38,40]

The Ga–S distance in **27** amounts to 2.093(2) Å which is significantly shorter than the sum of the covalent radii (2.27 Å, Table 1, Fig. 8) and shorter than typical Ga–S single bonds that the authors retrieved from the database.[37] Interestingly, synthetic access to **27** is also granted by conversion of $HB(pz^{tBu})_3Ga$ with the indium sulfur complex $HB(pz^{tBu})_3In(\eta^2\text{-}S_4)$ in a chalcogen exchange reaction (Scheme 18).[37,38] It is of note that for the indium *scorpionate* system no InS species with a

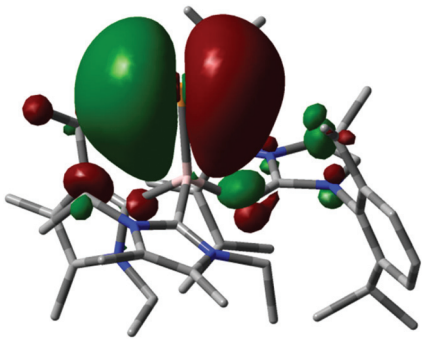

Fig. 7 Depiction of the HOMO−1 of **25**. Colours: Pink (aluminium), yellow (tellurium), blue (nitrogen), gray (carbon). Hydrogen atoms omitted.

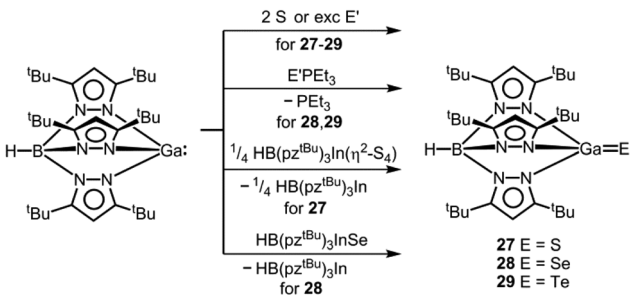

Scheme 18 Conversion of a trispyrazolylboryl gallium(I) compound to the gallium chalcogenides **27–29** (pz^{tBu} = 3,5-ditertbutyl-pyrazolyl, E' = Se or Te).

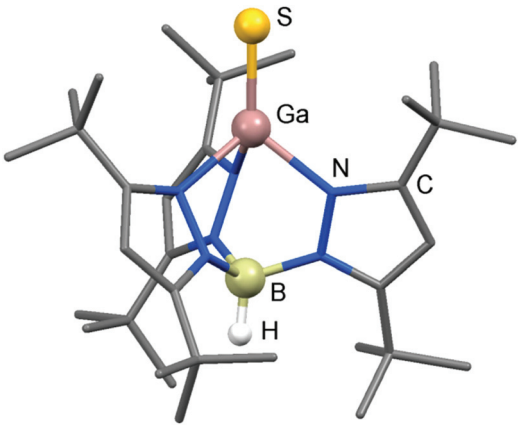

Fig. 8 Ball&stick model of the molecular structure of the trispyrazolylboryl gallium sulfide **27** in the solid state. Hydrogen atoms except on boron have been omitted. Pyrazolyl groups are depicted as a stick model.

terminal sulfur atom was described.[41] The heavier chalcogenides **28** and **29** exhibit gallium–chalcogen bond lengths of Ga–Se = 2.214(1) Å and Ga–Te = 2.422(1) Å.[38] These values are markedly below the sums of the respective covalent radii of 2.42 Å and 2.60 Å (Table 1). For comparison, the authors referenced 2.324(2) Å as the shortest average Ga–Se bond length observed for a complex compound. Similar to the gallium sulfide **27**, the gallium selenide **28** can be generated *via* conversion of $HB(pz^{tBu})_3Ga$ with $HB(pz^{tBu})_3InSe$ (**30**, *vide infra*, Scheme 18).[38,42] Furthermore, **28** and **29** can be furnished by implementation of $SePEt_3$ and $TePEt_3$ as a chalcogen source, respectively (Scheme 18). The bonding situation of the gallium–chalcogen interaction in $HB(pz^{tBu})_3GaE$ (**27–29**, E = S, Se, Te) was described as a composite of the resonance structures [Ga═E], [$^+$Ga–E$^-$], as well as [$^-$Ga≡E$^+$] and a main contribution of the zwitterionic form [$^+$Ga–E$^-$] was pronounced (*cf.* Fig. 1, **A**, **A′**, **A″**). However, no theoretical investigation was presented to verify this presumption. In fact, taking into account the theoretical studies on the nature of the Al═Te bond in **25**, as well as the Si═O bond in its sila-acylium ion congener (*vide supra*),[35,36] the weight of the canonical structure [Ga═E] should not be underrated.

Indium chalcogen double bond. As a scant example for an electron-precise complex that contains a potential indium chalcogen multiple bond, we found the scorpionate HB$(pz^{tBu})_3InSe$ (**30**) in the literature (*vide supra*, Scheme 19).[42]

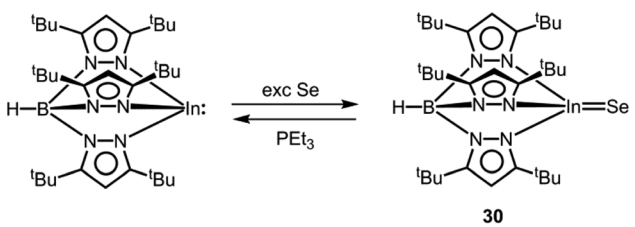

Scheme 19 Reaction of a trispyrazolylboryl indium(I) complex to the indium selenide **30** and regeneration of its precursor.

The compound was synthesized *via* conversion of $HB(pz^{tBu})_3In$ with elemental selenium (Scheme 19). Unlike the gallium congener **28**, it cannot be accessed *via* use of $SePEt_3$ as a selenium source. On the contrary, it readily transfers the chalcogen atom to PEt_3 (Scheme 19). The In–Se distance in **30** amounts to 2.376(1) Å which is considerably shorter than the sum of the covalent radii (2.62 Å, Table 1) and also reduced with respect to the mean In–Se single bond length that the authors determined to 2.65 Å.[42] Interestingly, the selenium atom in $HB(pz^{tBu})_3InSe$ (**30**) exchanges the chalcogen atom with $HB(pz^{tBu})_3Ga$ to produce $HB(pz^{tBu})_3In$ and $HB(pz^{tBu})_3GaSe$ (**28**, Scheme 18). Interestingly, the heavier analogue $HB(pz^{tBu})_3InTe$ was not obtained by the reaction of $HB(pz^{tBu})_3In$ with tellurium metal.[38] As outlined by Kuchta and Parkin, the indium–selenium interaction is composed of the three major resonance structures [In═Se], [$^+$In–Se$^-$] and [$^-$In≡Se$^+$] (*cf.* Fig. 1, **A**, **A′**, **A″**).[42] With regard to the susceptibility of $HB(pz^{tBu})_3InSe$ (**30**) towards chalcogen scavengers (*e.g.* $HB(pz^{tBu})_3Ga$, PEt_3), the strength of the InSe bond can be assessed as comparably low. In consideration of the higher atomic radius and the lower electronegativity of indium in comparison to gallium the contribution of the zwitterionic form [$^+$In–Se$^-$] is presumed to be significantly higher than for the gallium congener **28**. However, profound theoretical investigation (*e.g.* bond order, bond polarization, NRT study) would be required to shed more light on the bonding situation.

Conclusions

In summary this article has provided an overview on reports of electron-precise molecular complexes that contain a potential multiple bond between a group 13 element (M) and a chalcogen atom (E). No example for a purely kinetically stabilized multiple-bonded system of the type R–M═E or LB→M≡E (LB = Lewis base) that can be isolated in the condensed phase at ambient temperature is found in the literature (R = anionic substituent). However, various related species have been highlighted which exploit the concepts for thermodynamic stabilization *via* electron-donating and electron-accepting ancillary groups. Furthermore, isolation of the B≡O triple bond was achieved *via* electronic stabilization in the coordination sphere of platinum. The given examples demonstrate that the lability of the ME fragment increases with the polarization of the M–E bond, as well as the atomic radius of the group 13 element which is in accordance with the general expectation. Among the group 13 elements examples for B═E double bonds are most abundant and for thallium non-existent. Whether this is due to a bias in common research interests or results from a higher challenge for the isolation of respective substances is unclear. One way or the other, a higher demand for stabilization with rising metal character and larger coordination sphere of the element is to be expected. For the chalcogen group oxygen stands out in that no example has been reported in which it assumes a terminal position. Moreover, tellurium

lives up to its maverick position among the group 16 elements with only one double-bonded species reported.

Future studies should generally focus on applying bulkier ligand systems to grasp the intrinsically elusive parent ME species. The application of metal chalcogen multiple bonded systems in the field of Small Molecule Activation remains largely unexplored, but high prospect in this regard is implied by work of Pachaly and West, as well as Tokitoh and coworkers. Additionally, the capabilities of the gallium or indium chalcogen systems reported by Kuchta and Parkin which may function as chalcogen acceptor, as well as transfer reagents illustrate the tremendous potential of this compound class as an activator or catalyst.

Acknowledgements

Financial support of the WACKER Chemie AG, as well as the European Research Council (ERC Starting Grant: SILION 637394) is gratefully acknowledged.

References

1 (*a*) N. Kambe, K. Kondo, S. Morita, S. Murai and S. Sonoda, *Angew. Chem., Int. Ed. Engl.*, 1980, **19**, 1009; (*b*) I. Levin and D. Brandon, *J. Am. Ceram. Soc.*, 1998, **81**, 1995; (*c*) E. Y.-X. Chen and T. J. Marks, *Chem. Rev.*, 2000, **100**, 1391; (*d*) G. Busca, *Catal. Today*, 2014, **226**, 2; (*e*) W. Lee and S.-J. Park, *Chem. Rev.*, 2014, **114**, 7487; (*f*) M. Xia, K. Ding, F. Rao, X. Li, L. Wu and Z. Song, *Sci. Rep.*, 2015, **5**, 8548.

2 (*a*) H.-J. Himmel, A. J. Downs and T. M. Greene, *Chem. Rev.*, 2002, **102**, 4191; (*b*) A. Y. Timoshkin and H. F. Schaefer III, *J. Phys. Chem. A*, 2008, **112**, 13180; (*c*) N. A. Young, *Coord. Chem. Rev.*, 2013, **157**, 956; (*d*) T. Yang, D. S. N. Parker, B. B. Dangi, R. I. Kaiser, D. Stranges, Y.-H. Su, S.-Y. Chen, A. H. H. Chang and A. M. Mebel, *J. Am. Chem. Soc.*, 2014, **136**, 8387.

3 R. C. Fischer and P. P. Power, *Chem. Rev.*, 2010, **110**, 3877.

4 B. Pachaly and R. West, *J. Am. Chem. Soc.*, 1985, **107**, 2987.

5 Y. Shoji, N. Tanaka, K. Mikami, M. Uchiyama and T. Fukushima, *Nat. Chem.*, 2014, **6**, 498.

6 D. Vidovic, J. A. Moore, J. N. Jones and A. H. Cowley, *J. Am. Chem. Soc.*, 2005, **127**, 4566.

7 (*a*) B. Cordero, V. Gómez, A. E. Platero-Prats, M. Revés, J. Echeverría, E. Cremades, F. Barragán and S. Alvarez, *Dalton Trans.*, 2008, 2832; (*b*) R. S. Mulliken, *J. Chem. Phys.*, 1934, **2**, 782; (*c*) A. L. Allred and E. G. Rochow, *J. Inorg. Nucl. Chem.*, 1958, **5**, 264; (*d*) D. Bergmann and J. Hinze, *Angew. Chem., Int. Ed. Engl.*, 1996, **35**, 150.

8 (*a*) A. T. de Sousa, K. E. Bessler, S. S. Lemos, F. B. Gomes, G. A. Casagrande and E. Schulz Lang, *Z. Anorg. Allg. Chem.*, 2007, **633**, 771; (*b*) Y. Yamamoto, M. Takizawa, X.-Q. Yu and N. Miyaura, *Angew. Chem., Int. Ed.*, 2008, **47**, 928; (*c*) A. Budanow, E. von Grotthuss, M. Bolte and M. Wagner, *Tetrahedron*, 2016, **72**, 1477.

9 (*a*) C. Kleeberg, L. Dang, Z. Lin and T. B. Marder, *Angew. Chem., Int. Ed.*, 2009, **48**, 5350; (*b*) D. Franz, M. Bolte, H.-W. Lerner and M. Wagner, *Dalton Trans.*, 2011, **40**, 2433; (*c*) J. M. Breunig, A. Hübner, M. Bolte, M. Wagner and H.-W. Lerner, *Organometallics*, 2013, **32**, 6792.

10 Y. Wang, H. Hu, J. Zhang and C. Cui, *Angew. Chem., Int. Ed.*, 2011, **50**, 2816.

11 A. Solovyev, S. J. Geib, E. Lacôte and D. P. Curran, *Organometallics*, 2012, **31**, 54.

12 A. Del Grosso, E. R. Clark, N. Montoute and M. J. Ingleson, *Chem. Commun.*, 2012, **48**, 7589.

13 Y. Wang, M. Y. Abraham, R. J. Gilliard Jr., D. R. Sexton, P. Wei and G. H. Robinson, *Organometallics*, 2013, **32**, 6639.

14 T. Miyada and M. Yamashita, *Organometallics*, 2013, **32**, 5281.

15 M. A. Salomon, T. Braun and A. Penner, *Angew. Chem., Int. Ed.*, 2008, **47**, 8867.

16 Y. K. Loh, C. C. Chong, R. Ganguly, Y. Li, D. Vidovic and R. Kinjo, *Chem. Commun.*, 2014, **50**, 8561.

17 H. Braunschweig, K. Radacki and A. Schneider, *Science*, 2010, **328**, 345.

18 H. Braunschweig, K. Radacki and A. Schneider, *Chem. Commun.*, 2010, **46**, 6473.

19 S. Bertsch, J. Brand, H. Braunschweig, F. Hupp and K. Radacki, *Chem. – Eur. J.*, 2015, **21**, 6278.

20 N. Tokitoh, M. Ito and R. Okazaki, *Tetrahedron Lett.*, 1996, **37**, 5145.

21 H. Wang, J. Zhang, H. Hu and C. Cui, *J. Am. Chem. Soc.*, 2010, **132**, 10998.

22 J. Bauer, H. Braunschweig, A. Damme, J. O. C. Jimenez-Halla, T. Kramer, K. Radacki, R. Shang, E. Siedler and Q. Ye, *J. Am. Chem. Soc.*, 2013, **135**, 8726.

23 D. Franz, E. Irran and S. Inoue, *Angew. Chem., Int. Ed.*, 2014, **53**, 14264.

24 K. Jaiswal, B. Prashanth, S. Ravi, K. R. Shamasundar and S. Singh, *Dalton Trans.*, 2015, **44**, 15779.

25 P. Chen and C. Cui, *Chem. – Eur. J.*, 2016, **22**, 2902.

26 (*a*) G. Ferguson, J. F. Gallagher, M. McGrath, J. P. Sheehan, T. R. Spalding and J. D. Kennedy, *J. Chem. Soc., Dalton Trans.*, 1993, 27; (*b*) D. K. Roy, S. K. Bose, K. Geetharani, K. K. V. Chakrahari, S. M. Mobin and S. Ghosh, *Chem. – Eur. J.*, 2012, **18**, 9983; (*c*) A. Thakur, S. Sao, V. Ramkumar and S. Ghosh, *Inorg. Chem.*, 2012, **51**, 8322.

27 R. Köster, G. Seidel, W. Schüßler and B. Wrackmeyer, *Chem. Ber.*, 1995, **128**, 87.

28 (*a*) A. P. Shreve, R. Mulhaupt, W. Fultz, J. Calabrese, W. Robbins and S. D. Ittel, *Organometallics*, 1988, **7**, 409; (*b*) R. Benn, E. Janssen, H. Lehmkuhl, A. Rufińska, K. Angermund, P. Betz, R. Goddard and C. Krüger, *J. Organomet. Chem.*, 1991, **411**, 37; (*c*) M. D. Healy and A. R. Barron, *Angew. Chem., Int. Ed. Engl.*, 1992, **31**, 921; (*d*) M. D. Healy, M. R. Mason, P. W. Gravelle, S. G. Bott and A. R. Barron, *J. Chem. Soc., Dalton Trans.*, 1993, 441; (*e*) W. Clegg, E. Lamb, S. T. Liddle, R. Snaith and A. E. H. Wheatley, *J. Organomet. Chem.*, 1999, **573**, 305;

(*f*) Y. Yang, H. Li, C. Wang and H. W. Roesky, *Inorg. Chem.*, 2012, **51**, 2204; (*g*) C. Descour, T. J. J. Sciarone, D. Cavallo, T. Macko, M. Kelchtermans, I. Korobkov and R. Duchateau, *Polym. Chem.*, 2013, **4**, 4718; (*h*) L. Wang and L. Yang, *Acta Crystallogr., Sect. E: Struct. Rep. Online*, 2014, **70**, m352.

29 J. Li, X. Li, W. Huang, H. Hu, J. Zhang and C. Cui, *Chem. – Eur. J.*, 2012, **18**, 15263.

30 (*a*) R. J. Wright, A. D. Phillips and P. P. Power, *J. Am. Chem. Soc.*, 2003, **125**, 10784; (*b*) Y. Zhao, Y. Lei, Q. Dong, B. Wu and X.-J. Yang, *Chem. – Eur. J.*, 2013, **19**, 12059; (*c*) T. Agou, K. Nagata and N. Tokitoh, *Angew. Chem., Int. Ed.*, 2013, **52**, 10818; (*d*) K. Nagata, T. Agou and N. Tokitoh, *Angew. Chem., Int. Ed.*, 2014, **53**, 3881.

31 (*a*) C. Pluta, K.-R. Pörschke, C. Krüger and K. Hildenbrand, *Angew. Chem., Int. Ed. Engl.*, 1993, **32**, 388; (*b*) R. J. Wehmschulte, K. Ruhlandt-Senge, M. M. Olmstead, H. Hope, B. E. Sturgeon and P. P. Power, *Inorg. Chem.*, 1993, **32**, 2983.

32 D. Neculai, H. W. Roesky, A. M. Neculai, J. Magull, B. Walfort and D. Stalke, *Angew. Chem., Int. Ed.*, 2002, **41**, 4294.

33 (*a*) H. Zhu, J. Chai, V. Jancik, H. W. Roesky, W. A. Merrill and P. P. Power, *J. Am. Chem. Soc.*, 2005, **127**, 10170; (*b*) S. González-Gallardo, V. Jancik, R. Cea-Olivares, R. A. Toscano and M. Moya-Cabrera, *Angew. Chem., Int. Ed.*, 2007, **46**, 2895; (*c*) S. González-Gallardo, A. S. Cruz-Zavala, V. Jancik, F. Cortés-Guzmán and M. Moya-Cabrera, *Inorg. Chem.*, 2013, **52**, 2793.

34 (*a*) V. Jancik, Y. Peng, H. W. Roesky, J. Li, D. Neculai, A. M. Neculai and R. Herbst-Irmer, *J. Am. Chem. Soc.*, 2003, **125**, 1452; (*b*) A. P. Gómora-Figueroa, V. Jancik, R. Cea-Olivares and R. A. Toscano, *Inorg. Chem.*, 2007, **46**, 10749; (*c*) D. Franz, E. Irran and S. Inoue, *Dalton Trans.*, 2014, **43**, 4451; (*d*) D. Franz and S. Inoue, *Chem. – Eur. J.*, 2014, **20**, 10645.

35 D. Franz, T. Szilvási, E. Irran and S. Inoue, *Nat. Commun.*, 2015, **6**, 10037.

36 S. U. Ahmad, T. Szilvási, E. Irran and S. Inoue, *J. Am. Chem. Soc.*, 2015, **137**, 5828.

37 M. C. Kuchta and G. Parkin, *J. Chem. Soc., Dalton Trans.*, 1998, 2279.

38 M. C. Kuchta and G. Parkin, *Inorg. Chem.*, 1997, **36**, 2492.

39 F. T. Edelmann, *Angew. Chem., Int. Ed.*, 2001, **40**, 1656.

40 M. C. Kuchta, J. B. Bonanno and G. Parkin, *J. Am. Chem. Soc.*, 1996, **118**, 10914.

41 M. C. Kuchta and G. Parkin, *Main Group Chem.*, 1996, **1**, 291.

42 M. C. Kuchta and G. Parkin, *J. Am. Chem. Soc.*, 1995, **117**, 12651.